



Effect of two-dimensional ultrasonic rolling on grain size and micro-hardness of 7075 aluminum alloy

Jianxin Zheng¹ · Hongwei Liu¹ · Yuanchao Ren¹ · Lixin Zhu¹

Received: 1 July 2019 / Accepted: 4 November 2019 / Published online: 23 November 2019
© Springer-Verlag London Ltd., part of Springer Nature 2019

Abstract

Two-dimensional ultrasonic surface rolling process (TDUSR) is an effective method to improve fatigue, wear, and corrosion resistance of materials by producing strain hardening and changing stress state and microstructure. In this paper, the experiment and finite element simulation of two-dimensional ultrasonic surface rolling 7075 aluminum alloy were carried out to study the evolution of the microstructure and the relationship between the surface grain size and micro-hardness. Deform was redeveloped on the basis of grain refinement model to simulate the change of grain size of 7075 aluminum alloy after TDUSR treatment. The micro-hardness and grain size obtained by TDUSR were analyzed using micro-hardness tester and XRD diffractometer. The relationship between the grain size and micro-hardness was established based on the experimental results. The simulation and experimental results showed that the grain size in the rolled region decreased greatly after TDUSR treatment. And the grain size refined from micron to nanometer, forming a gradient nanocrystalline structure along the radial direction. The grain refinement might be caused by the comprehensive influence of the surface equivalent stress and the equivalent strain rate when the static load was less than 150 N. When the static load exceeded 150 N, the plastic deformation temperature also had a certain effect on the grain refinement. TDUSR treatment can promote the preferred grain orientation and change the microstructure in the rolled surface layer. The inverse Hall-Petch phenomenon existed in the nanostructured surface layer, and the surface micro-hardness increased with the increment of the grain size.

Keywords Two-dimensional ultrasonic rolling · 7050 aluminum alloy · Grain refinement · Micro-hardness · Inverse Hall-Petch phenomenon

1 Introduction

In recent years, 7075 aluminum alloy has been widely applied in many engineering fields, including aerospace, automobile, and weapons [1, 2]. However, the parts made of 7075 aluminum alloy will be subjected to the cyclic load during their working, which might lead to surface abrasion and failure, even result in early failure and greatly reduce their service life [3, 4]. Therefore, it is particularly important to improve the surface fatigue and wear properties of the parts and prolong their service life for the reliable and safe operation of these parts [5, 6].

Surface hardening technology introduces severe plastic deformation (SPD) on the surface of metal parts to change the microstructure, increase the dislocation density, and induce a gradient nanocrystalline structure in the surface layer. Thereby, it can improve the yield strength, the fatigue resistance, and wear resistance of the parts, and ultimately prolong its service life [7–10]. Ultrasonic surface rolling (USR) is a high efficiency and quality surface hardening technique. In USR, SPD occurs at the surface of the part under the high strain rates when the ball impacts the part with high frequency, which induces nanocrystalline grains in a certain depth, denser surface structure, and higher hardness of the part, and then improve the fatigue resistance and wear resistance of materials and prolong their service life [11–13]. Zhang et al. [14] investigated 17-4PH stainless steel subjected to USR treatment, they found that the surface grain of parts was refined, and the surface micro-hardness was increased by 20% compared with the initial state. Zhao et al. performed

✉ Jianxin Zheng
zhengjx@hpu.edu.cn

¹ College of Mechanical & Power Engineering, Henan Polytechnic University, Jiaozuo 454003, People's Republic of China

ultrasonic rolling treatment on 300 M ultra-high strength steel, and they found that the grain size of the surface layer decreased and the dislocation density increased, a hardening layer of about 140 μm was formed on the surface of the specimen, the average hardness of the surface layer was 876 $\text{HK}_{0.25}$, and the fatigue life was prolonged [15]. Yin et al. investigated the effect of ultrasonic surface rolling on the wear behavior of Inconel 690 alloy tubes, and the results showed that the improvement of wear resistance of 690 alloy was attributed to the decrease of grain size and the increase of micro-hardness of 690 alloy [16].

Experiments show that two-dimensional ultrasonic surface rolling (TDUSR) treatment can significantly improve surface micro-hardness. Meanwhile, multidimensional peening is beneficial to the plastic deformation in different directions, and also helpful to the realization of surface nanocrystallization [17]. In this work, the experiment and finite element simulation of the shaft made of 7075 aluminum alloy in the process of TDUSR were carried out. The evolution of the grain size and the micro-hardness of the shaft under different static loads were studied. And the relationship between the grain size and the micro-hardness of the shaft treated by TDUSR was explored.

2 Principles of TDUSR

The processing sketch map of TDUSR is shown in Fig. 1. The shaft is mounted on the lathe and rotates at the speed of n . The ultrasonic acoustic system is mounted on the tool holder by the gripper block. The transducer transforms the ultrasonic frequency signal generated by the ultrasonic power supply into one-dimensional mechanical vibration. The horn with skewed slots then transforms the mechanical vibration into longitudinal-torsional vibration, and amplifies the vibration amplitude and transmits the vibration to the smooth roller. The roller then acts on the shaft under the longitudinal ultrasonic vibration A

along the radial direction and the torsional ultrasonic vibration B around the radial direction. Besides the two-dimensional ultrasonic peening, the roller also acts on the shaft with certain static load F_s and moves along the axis of the shaft with the feed-rate f_r .

In the TDUSR process, the combined action of static load and ultrasonic peening leads to severe plastic deformation on the shaft surface. The longitudinal and torsional ultrasonic vibration of the roller causes the surface grains of the material to undergo different stress fields under the dual action of normal stress and shear stress. So the dislocation slip movement of the original grains occurs at high energy state. With the accumulation of plastic deformation, the coarse crystal grains evolve into fine grains through the dislocation evolution, and strain hardening is produced in the surface layer of the material so as to improve the hardness of the part.

3 Experiment and finite element simulate

3.1 Experimental procedures

The specimen used in this study was a shaft made of 7075-T651 aluminum alloy with a diameter of 80 mm. It was treated by repeated multi-directional hot forging, and then solution treated at 450–480 $^{\circ}\text{C}$ for 30 min, aged at 120 $^{\circ}\text{C}$ for 6 h, then re-aged at 160 $^{\circ}\text{C}$ for 24 h, and stretched to 1–3% plastic strain to eliminate the residual thermal stress. And its chemical composition is presented in Table 1. The specimen was pretreated by turning, and turning parameters were as follows: the rotating speed n was 900 r/min, the feed-rate f_r was 0.24 mm/r, and the cutting depth a_p was 0.2 mm. After turning, the diameter of the specimen was 78 mm, the surface micro-hardness was about 141 $\text{HV}_{0.1}$, and the minimum grain size of the surface layer was about 0.342 μm .

The experimental setup is shown in Fig. 2. The specimen was clamped on the lathe CA6140B/A. The two-dimensional ultrasonic acoustic system was mounted on the lathe carriage, and the roller with a diameter of 12 mm made of YG8

Fig. 1 Processing sketch map of TDUSR

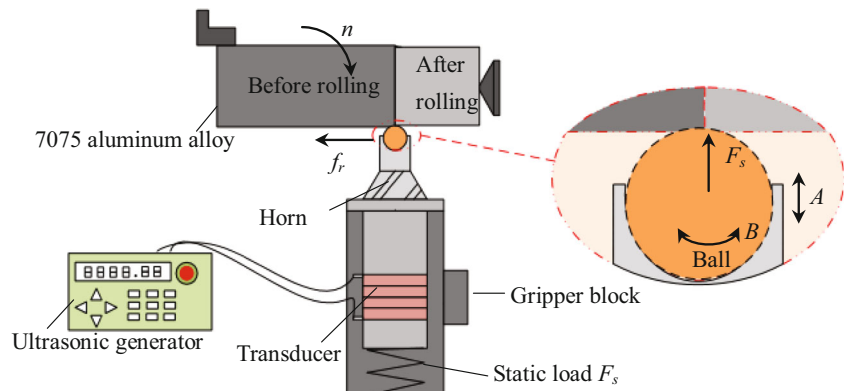


Table 1 Chemical composition of 7075 aluminum alloy (wt%)

Si	Fe	Cu	Mn	Mg	Cr	Zn	Ti	Al
0.23	0.331	1.67	0.265	2.52	0.204	5.81	0.049	else

cemented carbide moved with the lathe carriage. In this experimental procedure, the roller vibrated with a resonant frequency $f = 25.6$ kHz, the longitudinal amplitude $A = 3.5$ μm , and the torsional ultrasonic vibration $B = 1$ μm . The rolling parameters in TDUSR were set as follows: the rotating speed n was 710 r/min and the feed-rate f_r was 0.15 mm/r, the static load F_s was 100 N, 125 N, 150 N, 175 N, and 200 N, respectively.

After TDUSR treatment, the shaft was cut into the specimen with a longitudinal section 20 mm \times 20 mm by wire electrical discharge machining (WEDM) and then polished by the sandpaper with #1200 for the subsequent tests. The XRD diffraction spectrum of the specimen was measured by D8 ADVANCE X-ray diffractometer, and the obtained XRD patterns were analyzed by Jade software to calculate the grain size of the specimen. The surface hardness of the specimen was measured using a HV-1000 micro-hardness tester under a load of 0.1 N and a loading time of 10 s. The measurement was repeated three times and the average was computed as the final hardness value.

3.2 Finite element simulation

In order to analyze the evolution of grain size induced by SPD in TDUSR process, software Deform was applied to simulate the TDUSR process for the 7075 shaft.

In TDUSR, the ultrasonic peening of the ball on the shaft will generate plastic deformation with high strain rate. As the rolling depth is small and the rotating speed is low, TDUSR is characterized by low strain, high strain rate, and common temperature. So the built-in dynamic recrystallization model is not suitable for the simulation, and it is necessary to conduct secondary development for the software Deform to simulate

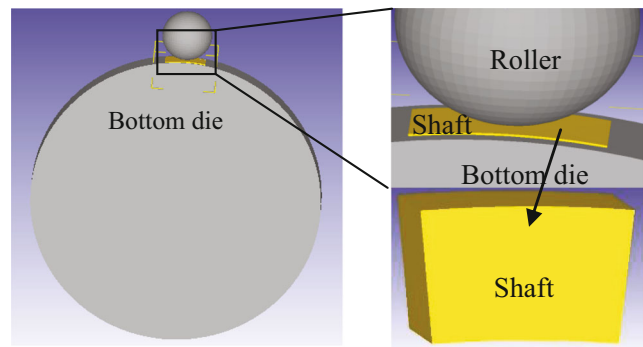


Fig. 3 Assembly drawing of geometric model

the evolution of the grain size of 7075 aluminum alloy treated by TDUSR.

3.2.1 Secondary development of software Deform

In the secondary development of software Deform, the `usr-msh.f` subroutine is used to define the data transmission between the moving steps and the export of the simulation results; the `usr-upd.f` subroutine is used to edit the grain refinement model. The grain refinement model is described as follows.

7075 aluminum alloy has face-centered cubic crystal (FCC) structure. In the plastic deformation process, when the dislocation density of the material with FCC structural changes, its microstructure changes. While the stress and the strain rate are necessary conditions for the change of the dislocation density. The relationship between the stress σ and the plastic strain rate $\dot{\epsilon}$ caused by the dislocation can be briefly described by Arrhenius formula [18]:

$$\left(\frac{\dot{\epsilon}}{\dot{\epsilon}_0}\right)^{1/m} = \left(\frac{\sigma}{\tilde{\sigma}}\right) \tag{1}$$

where $\dot{\epsilon}$, $\dot{\epsilon}_0$, σ , $\tilde{\sigma}$, $\tilde{\sigma}$ and $1/m$ are the strain rate, the reference value of the strain rate, the stress, the flow stress, and the sensitive coefficient of the strain rate, respectively, and $1/m$ is deduced to be 0.25 in this work [18, 19].

Fig. 2 TDUR experiment setup

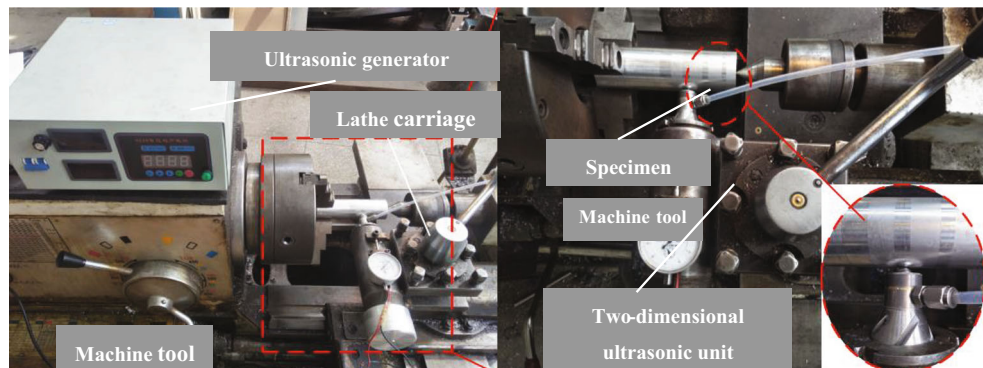


Table 2 Physical properties of 7075 and YG8

Materials	E (GPa)	ρ (kg/m ³)	μ	σ_b (MPa)	σ_s (MPa)	G (GPa)	b (nm)
7075	71	2820	0.33	575	503	26.9	0.286
YG8	600	14500	0.21				

The relationship between the dislocation density ρ_t and the flow stress $\tilde{\sigma}$ can be expressed as

$$\tilde{\sigma} = MaGb\sqrt{\rho_t} \quad (2)$$

where M is the Taylor factor, which is 2.65 in this work, α is a constant and is 0.25, G is the shear modulus, b is the Burgers vector, and ρ_t is the dislocation density.

The relationship between the dislocation density ρ_t and the grain size d is described as follows [19]:

$$d = \frac{k}{\sqrt{\rho_t}} \quad (3)$$

where k is a proportionality constant and $k = 30$ [19].

So

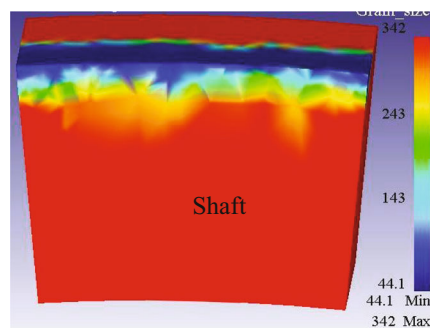
$$d = \frac{kMaGb}{\sqrt{\varepsilon_0}} A \quad (4)$$

where A is the ratio of the equivalent strain rate to the equivalent stress, $A = \frac{\sqrt{\varepsilon_0}}{\sigma}$.

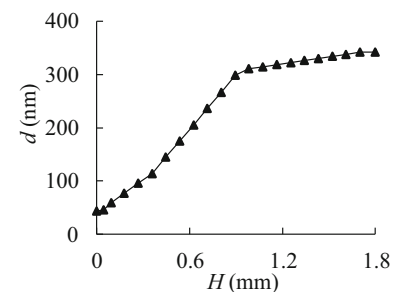
3.2.2 Simulation process

The geometric models for TDUSR were established as shown in Fig. 3. The shaft was made of 7075 aluminum alloy with a diameter of 78 mm, and the roller was made of cemented carbide YG8 with a sphere diameter of 12 mm. The rotation of the shaft was driven by the bottom die. To simplify the simulation, the shaft was cut into a curved plate with a thickness of 5 mm.

Fig. 4 Grain size distribution. **a** Distribution nephogram of grain size. **b** Grain size along the radial direction



(a) Distribution nephogram of grain size



(b) Grain size along the radial direction

The constitutive model of 7075 aluminum alloy was established based on the stress-strain data curve obtained from the reference [20]. The mechanical properties of 7075 and YG8 were shown in Table 2. Used the default tetrahedron shape of the element to mesh the models, and then refined the rolling region.

The movement of the shaft, the roller, and the bottom die was defined based on Fig. 1. The feed-rate f_r , rotating speed n , ultrasonic vibration frequency f , torsional amplitude A , torsional amplitude B , and static pressures F required to simulate were set as follows: $f_r = 0.15$ mm/r, $n = 710$ r/min, $f = 25.6$ kHz, $A = 3.5$ μ m, $B = 1$ μ m, and $F = 100, 125, 150, 175, 200$ N, respectively. When the simulation setup was completed, the operation was performed.

E , elasticity modulus; ρ , density; μ , Poisson ratio; σ_b , tensile strength; σ_s , yield strength; G , shear modulus; b , Burgers vector

4 Results and discussion

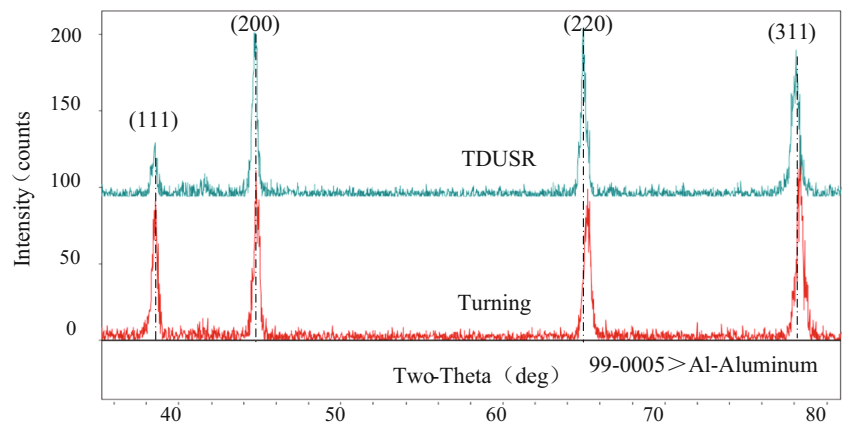
4.1 FEA results

The simulated grain size distribution under the static load 200 N is presented in Fig. 4. Figure 4(a) shows the distribution nephogram of the grain size in the rolling region and Fig. 4(b) describes the grain size along the radial direction in the rolling region. Figure 4 shows that the grain size of the rolled surface region decreases significantly from 342 to 44.1 nm after TDUR treatment, and a gradient nanograined surface layer is formed along the radial direction. The grain size gradually increases beneath the surface until it is equal to the original grain size.

4.2 Experimental results

The XRD patterns of the specimen obtained by turning and TDUSR under the static load 200 N are presented in Fig. 5. Figure 5 shows that there are no new Bragg diffraction peaks appear after TDUSR treatment in contrast to turning, and the

Fig. 5 XRD diffraction peak of work-piece surface



indices of crystal face for each peak are (111), (200), (220), and (311), respectively. The intensity of the diffraction peaks in the crystal faces (111) and (311) decrease, which is attributed to the preferred orientation of the grains induced by SPD. The diffraction peaks of the crystal faces (200), (220), and (311) are obviously shifted, and these shifts are caused by the space change of crystal faces due to the plastic deformation.

Contrasting with turning, the position variance of the diffraction peaks at the same angle in the XRD pattern indicates that TDUSR treatment produces the dislocation glide, grain refinement, and lattice rotation to some extent. TDUSR treatment can promote the preferred grain orientation and change the microstructure in the surface layer, then improve the surface micro-hardness and the corrosion-resistant and fatigue properties of the specimen [21].

The XRD spectrum of the samples was analyzed by MDI-Jade6.0 software, and the grain size was calculated by the half-peak width of the diffraction peak based on Debye-Scherrer equation. After processed by TDUSR under different static loads, the surface grain sizes obtained from the experiment are in comparison with the simulation, seen from Fig. 6.

Figure 6 shows that the experimental values (*EV*) are in good agreement with the simulation values (*SV*), with an error less than 8.1%. The grain size is between 36.7 and 64.5 nm. With the increment of the static load, the grain size increases first, then decreases, and then increases. And the grain size under the static load 175 N is a little smaller than that of 200 N.

The measured surface micro-hardness of the specimen treated by TDUSR is shown in Fig. 7. The surface micro-hardness increases to a certain extent compared with 141 HV_{0.1} after turning. When the static load increases from 100 to 150 N, the surface micro-hardness increases from 156.2 to 176.1 HV_{0.1}, increasing by 24.8%. Then when the static load increases to 175 N and 200 N, the surface micro-hardness value decreases to a closer value (159.3 HV_{0.1} and 160.8 HV_{0.1}, respectively).

4.3 Discussion

The grain refinement is induced by SPD after TDUSR treatment, and SPD may lead to the change of the surface stress and the strain rate. In order to analyze the

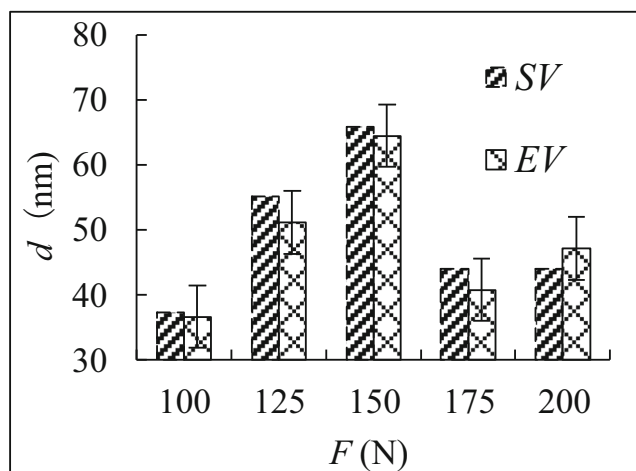


Fig. 6 Effect of static load on grain size

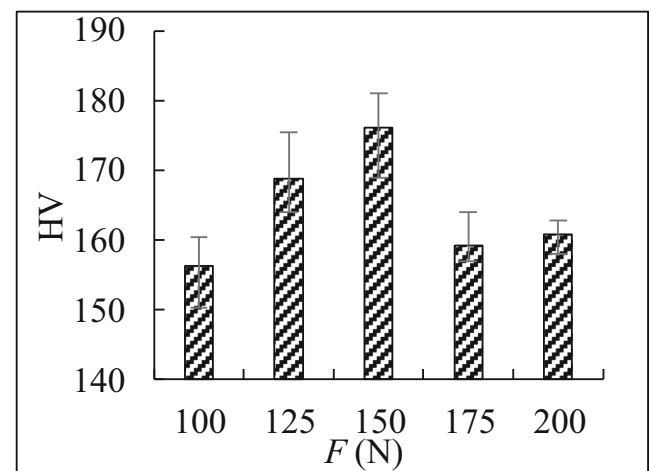


Fig. 7 Effect of static load on micro-hardness

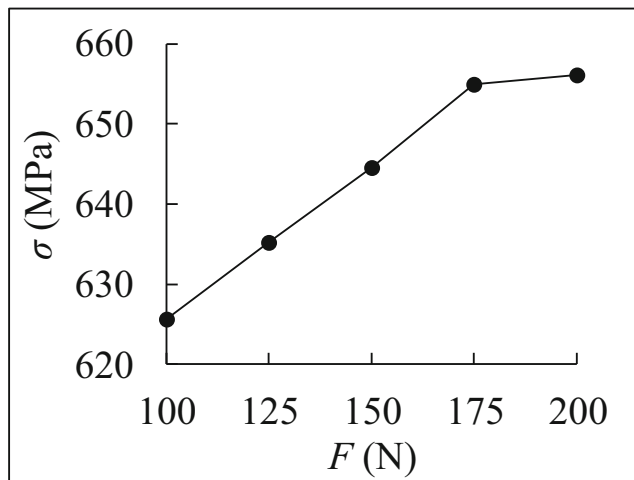


Fig. 8 Surface equivalent stress

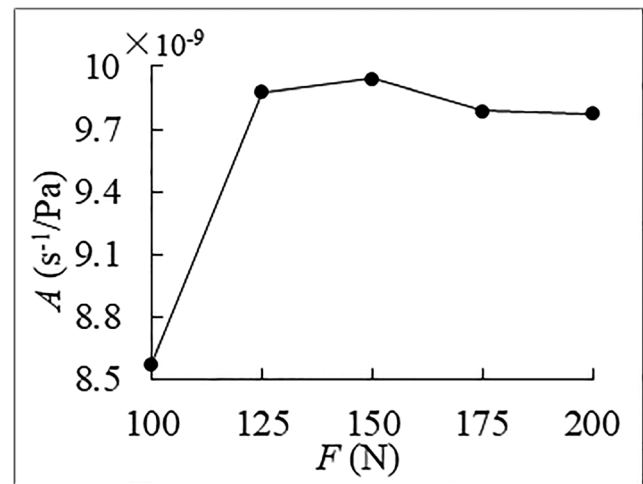


Fig. 10 Equivalent strain rate to equivalent stress ratio curve

equivalent stress σ and the strain rate $\dot{\varepsilon}$ under different static load, the surface equivalent stress σ and strain rate $\dot{\varepsilon}$ were extracted from the finite element simulation results, as shown in Figs. 8 and 9.

Figure 8 shows that the surface equivalent stress of 7075 aluminum alloy after TDUSR treatment is greater than the yield strength (503 MPa) and increases with the increment of the static load. Figure 9 shows the surface equivalent strain rate increases greatly and then slowly with the increment of the static load. The surface equivalent strain rate changes little when the static load exceeds 150 N.

The change of the ratio A of the equivalent strain rate to the equivalent stress under different surface static load is shown in Fig. 10. A increases when the static load increases from 100 to 150 N. And when the static load increases from 150 to 200 N, the change of the ratio A is not obvious.

Compared to Fig. 6, the variation trend of the grain size under different static load agrees with that of the ratio A when the static load increases from 100 to 150 N, and disagrees

when the static load increases from 150 to 200 N. The simulated maximum temperature in the rolling region for 7075 treated by TDUSR is shown in Fig. 11. Figure 11 shows that when the static load increases to 175 N, the maximum surface temperature in the rolling region increases sharply. The flow stress of aluminum 7075-T651 was strongly sensitive to temperature compared with strain rate, the flow stress reduced with the increase of temperature [20]. In general, the increment of deformation temperature leads to the decrement of the shear modulus G and the flow stress $\tilde{\sigma}$, the dynamic recovery and dynamic recrystallization are more likely to occur. On the other hand, the increment of deformation temperature may cause severe dislocation annihilate and lead to coarse grain. So we deduce that when the static load is less than 150 N, the grain refinement might be caused by the comprehensive influence of the surface equivalent stress and the equivalent strain rate. When the static load exceeds 150 N, the plastic deformation temperature also has certain effect on the grain refinement.

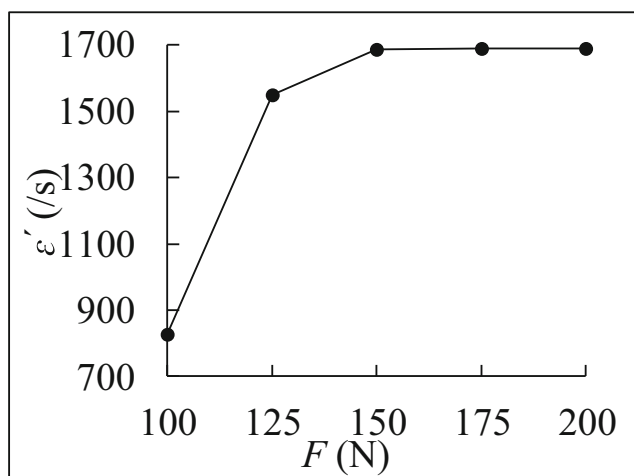


Fig. 9 Surface equivalent strain rate

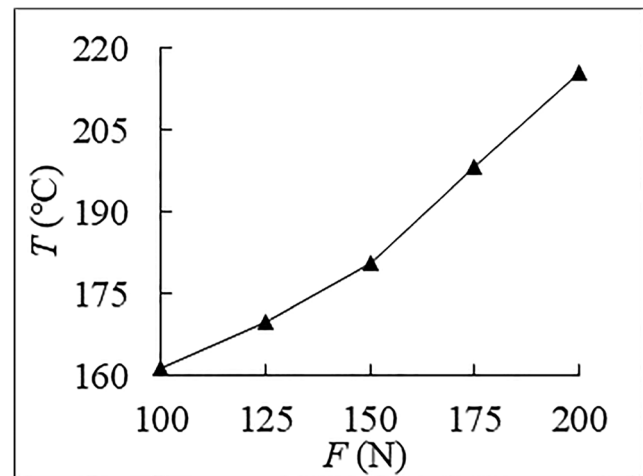
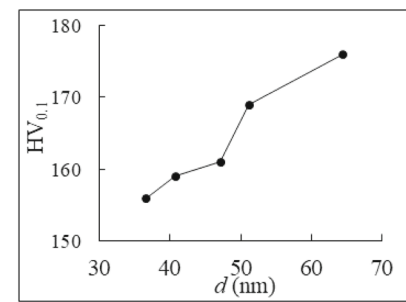
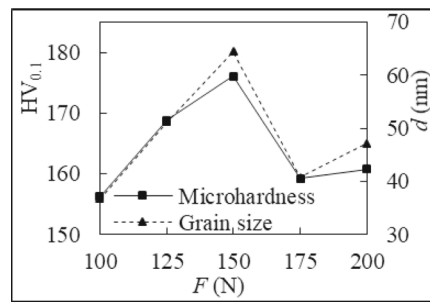


Fig. 11 Simulated maximum surface temperature

Fig. 12 The relationship between grain size and micro-hardness. **a** Grain size and micro-hardness under different static load. **b** Trend of grain size and micro-hardness



(a) Grain size and micro-hardness under different static load (b) Trend of grain size and micro-hardness

After TDUR treatment, the grain refinement and compacted dislocation density caused by SPD may make the surface microstructure closer than its original surface, which contributes to the improvement of the surface micro-hardness. The relationship between the grain size and the micro-hardness is shown in Fig. 12. Figure 12 shows that the influences of the static load on the grain size and the micro-hardness are almost the same, and the surface micro-hardness increases with the increment of the grain size, which shows that the inverse Hall-Petch phenomenon also exists in the nanostructured surface layer [22].

Compared to turning, the surface grain dislocation motion will be promoted by SPD and the high strain rate in the process of TDUSP, which results in the grain refinement and the increment of the slip deformation resistance, and then improves the surface micro-hardness. After TDUSR treatment, the grain size of the material reduces to nanocrystalline size. The smaller the grain size is, the more the number of the grain boundaries is. It may hinder the grain slip deformation, produce the grain boundary coordination and grain rotation. And the deformation energy required and the resistance are reduced, which results in the lower hardness of the material. Therefore, the inverse Hall-Petch phenomenon occurs in the rolled surface layer.

The relationship-similar to the Hall-Petch relation [23] between the micro-hardness and the grain size of 7075 aluminum alloy treated by TDUSR was established by using regression analysis method, as shown in the following formula:

$$HV = HV_0 + 0.059d^{1.538} \quad (6)$$

where HV_0 is the original surface micro-hardness (141 $HV_{0.1}$), d is the grain size (nm), and HV is the surface micro-hardness of the processed specimen.

Comparing the measured results with the calculated based on the above model, the maximum error is no more than 1.8%, which indicates that the above model may be used to predict the micro-hardness based on the grain size in TDUSR.

5 Conclusion

In TDUSR, the roller exerts high frequency longitudinal peening and torsional rolling on the surface of the 7075 aluminum alloy shaft, and induces severe plastic deformation in different directions. The micro-structure changes and the strain hardening occurs, which leads to the grain refinement and micro-hardness improvement.

- 1) The simulation results show that the grain size of the rolled surface region decreases significantly from 342 to 44.1 nm after TDUR treatment, and a gradient nanograined surface layer is formed along the radial direction. The grain refinement might be caused by the comprehensive influence of the surface equivalent stress and the equivalent strain rate when the static load is less than 150 N. When the static load exceeds 150 N, the plastic deformation temperature also has a certain effect on the grain refinement.
- 2) Compared to turning, the diffraction peaks of the crystal faces (200), (220), and (311) are obviously shifted to the left, which indicates that TDUSR treatment can promote the preferred grain orientation and change the microstructure in the rolled surface layer.
- 3) The experimental results of the grain size are in good agreement with the simulation results, with an error less than 8.1%. The surface grain size decreases significantly and the surface micro-hardness increases obviously after TDUR treatment, and they increase first and then decrease with the increment of the static load.
- 4) The inverse Hall-Petch phenomenon exists in the nanostructured surface layer, and the surface micro-hardness increases with the increment of the grain size. The inverse mathematical Hall-Petch model constructed from the experimental results can well describe the relationship between the surface micro-hardness and the surface grain size of 7075 aluminum alloy after TDUR treatment.

Funding information This work was supported by the National Natural Science Foundation of China (grant numbers 51005071, 51575163) and

the Key Scientific Research Project for the Universities in Henan Province, China (grant number 16A460006).

References

- Dobosy A, Gáspár M, Török I (2018) Resistance spot welding of 7075 aluminum alloy[J]. *Vehicle and Automotive Engineering* 2: 679–693
- Fernando C, Ruano OA (2018) Superplasticity of aerospace 7075 aluminum alloy obtained by severe plastic deformation[J]. *Defect and Diffusion Forum* 385:39–44
- Pandey V, Chattopadhyay K, Santhi Srinivas NC, Singh V (2017) Effect of stress relieving treatment on low cycle fatigue behavior of USSP treated 7075 aluminum alloy[J]. *Materials Science and Engineering* 194:012037
- Delgado P, Cuesta II, Alegre JM, Díaz A (2016) State of the art of deep rolling[J]. *Precision Engineering* 46:1–10
- Xu X, Liu D, Zhang X, Liu C, Liu D, Zhang W (2019) Influence of ultrasonic rolling on surface integrity and corrosion fatigue behavior of 7B50-T7751 aluminum alloy[J]. *International Journal of Fatigue* 125:237–248
- Lu L, Sun J, Li L, Xiong Q (2016) Study on surface characteristics of 7050-T7451 aluminum alloy by ultrasonic surface rolling process[J]. *The International Journal of Advanced Manufacturing Technology* 87(9-12):2533–2539
- Li G, Qu S, Pan Y, Li X (2016) Effects of the different frequencies and loads of ultrasonic surface rolling on surface mechanical properties and fretting wear resistance of HIP Ti–6Al–4 V alloy[J]. *Applied Surface Science* 389(15):324–334
- Rajabi F, Zarei-Hanzaki A, Eskandari M, Khoddam S (2013) The effects of rolling parameters on the mechanical behavior of 6061 aluminum alloy[J]. *Materials Science & Engineering A* 578(31): 90–95
- Muñoz-Cubillos J, Coronado JJ, Rodríguez SA (2017) Deep rolling effect on fatigue behavior of austenitic stainless steels[J]. *International Journal of Fatigue* 95:120–131
- Ramos R, Ferreira N, Ferreira JAM, Capela C, Batista AC (2016) Improvement in fatigue life of Al 7475-T7351 alloy specimens by applying ultrasonic and micro-shot peening[J]. *International Journal of Fatigue* 92(1):87–95
- Cheng M, Zhang D, Chen H, Wei Q, Li J (2016) Surface nanocrystallization and its effect on fatigue performance of high-strength materials treated by ultrasonic rolling process[J]. *The International Journal of Advanced Manufacturing Technology* 83(1-4):123–131
- She D, Yue W, Du Y, Fu Z, Wang C, Liu J (2015) Vacuum tribological properties of titanium with a nano-crystalline surface layer[J]. *Tribology Letters* 57:1
- Ben Moussa N, Gharbi K, Chaieb I, Ben FN (2019) Improvement of AISI 304 austenitic stainless steel low-cycle fatigue life by initial and intermittent deep rolling[J]. *The International Journal of Advanced Manufacturing Technology* 101:435–449
- Zhang Q, Hu Z, Su W, Zhou H, Liu C, Yang Y, Qi X (2017) Microstructure and surface properties of 17-4PH stainless steel by ultrasonic surface rolling technology[J]. *Surface and Coatings Technology* 321:64–73
- Zhao W, Liu D, Zhang X, Zhou Y, Zhang R, Zhang H, Ye C (2018) Improving the fretting and corrosion fatigue performance of 300M ultra-high strength steel using the ultrasonic surface rolling process[J]. *International Journal of Fatigue* 121:30–38
- Yin M, Cai Z, Zhang Z, Yue W (2019) Effect of ultrasonic surface rolling process on impact-sliding wear behavior of the 690 alloy[J]. *Tribology International*.
- Gavrilova TM (2008) Contact friction in the deformation zone during ultrasonic surface plastic deformation[J]. *Russian Engineering Research* 28(8):764–768
- Estrin Y, Mecking H (1984) A unified phenomenological description of work hardening and creep based on one-parameter models[J]. *Acta Metallurgica* 32(1):57–70
- Chul Baik S, Estrin Y, Seop Kim H, Jörg HR (2003) Dislocation density-based modeling of deformation behavior of aluminium under equal channel angular pressing[J]. *Materials Science & Engineering A* 351(1-2):86–97
- Wu Y, Li S, Hou B, Yu Z (2013) Dynamic flow stress characteristics and constitutive model of aluminum 7075-T651[J]. *The Chinese Journal of Nonferrous Metals*[J] 3:658–665
- Wang Z, Xiao Z, Huang C, Wen L, Zhang W (2017) Influence of ultrasonic surface rolling on microstructure and wear behavior of selective laser melted Ti-6Al-4V Alloy[J]. *Materials* 10(10):1203
- Pande CS, Cooper KP (2009) Nano-mechanics of Hall–Petch relationship in nanocrystalline materials[J]. *Progress in Materials Science* 54(6):689–706
- Sato YS, Urata M, Kokawa H, Ikeda K (2003) Hall–Petch relationship in friction stir welds of equal channel angular-pressed aluminum alloys[J]. *Materials Science & Engineering* 354(1-2):298–305

Publisher's note Springer Nature remains neutral with regard to jurisdictional claims in published maps and institutional affiliations.